Vidal, Y. and Huerta, A., Goal oriented error estimation for the Element Free Galerkin method, *Lecture Notes on computational science and engineering*, Vol. 57, pp. 265-282, 2007

Goal oriented error estimation for the Element Free Galerkin method

Yolanda Vidal and Antonio Huerta

Laboratori de Càlcul Numèric, Departament de Matemàtica Aplicada III,
Universitat Politècnica de Catalunya, Jordi Girona 1, E-08034 Barcelona, Spain
{yolanda.vidal,antonio.huerta}@upc.edu

Summary. A novel approach for implicit residual-type error estimation in mesh-free methods is presented. This allows to compute upper and lower bounds of the error in energy norm with the ultimate goal of obtaining bounds for outputs of interest. The proposed approach precludes the main drawbacks of standard residual type estimators circumventing the need of flux-equilibration and resulting in a simple implementation that avoids integrals on edges/sides of a domain decomposition (mesh). This is especially interesting for mesh-free methods.

Key words: Element Free Galerkin, mesh-free methods, error estimation, engineering outputs, residual based estimators.

1 Introduction

Assessment of functional outputs of the solution (goal-oriented error estimation) in *computational mechanics* problems is a real need in standard engineering practice. In particular, end-users of finite elements, finite differences or mesh-free codes are interested in obtaining bounds for quantities of engineering interest. Techniques providing these bounds require using error estimators in the energy norm of the solution. Bounds for quantities of interest (functional outputs) are recovered combining upper and lower bounds of the energy error for both the original problem (primal) and a dual problem (associated with the selected functional output) [21, 1, 20].

It is also important to note that bounds for the energy and for quantities of interest are usually obtained with respect to a reference solution (associated with a much larger space of approximation). Bounds for the exact solution of the boundary value problem as presented in [3, 26, 22] are not addressed here.

The need of obtaining reliable upper and lower bounds of the error for quantities of interest has motivated the use of residual error estimators, which are currently the only type of estimators ensuring bounds for the error. Classical residual type estimators, which provide upper bounds of the error, require

flux-equilibration procedures (*hybrid-flux* techniques) to properly set boundary conditions for local problems [14, 1]. Flux-equilibration requires a domain decomposition, which is natural in finite elements but not in mesh-free methods. And, moreover, it is performed by a complex algorithm, strongly dependent on the finite element type and requiring a data structure that is not natural in a standard finite element code. Thus highly embedded in the finite element domain decomposition.

The idea of using flux-free estimators, based on the partition-of-the-unity concept and using local subdomains different than elements, has been already proposed in [4, 16, 18, 23] for finite elements. The main advantage of the flux-free approach is the simplicity in the implementation. Obviously, this is especially important in the 3D case.

From the mesh-less point of view, another advantage is the fact that the local subdomains where the error equation is solved are the support of the functions characterizing the partition of unity. This is a concept that also exists in mesh-free methods and thus the extension is possible. Moreover, boundary conditions of the local problems are trivial and the usual data structure of a code is directly employed.

In the last few years, some research has been devoted to develop error estimation procedures for mesh-free methods. Duarte and Oden [7] derived an explicit residual error estimator for the h-p cloud method. Liu *et al* [15] used a wavelet solution as an error indicator in an algorithm where multiple-scale adaptive refinement had been introduced. Chung and Belytschko [5] adapted the FEM stress projection technique for error analysis in Element Free Galerkin (EFG). Gavete *et al* [10] proposed a sort of recovery-based error estimate, which presents the standard drawbacks of these methods. None of these approaches was able to compute bounds of the energy error. Thus, the assessment of bounds and functional outputs is still an open topic in mesh-free methods.

To the authors knowledge implicit residual based estimators have not been proposed for mesh-free methods. However, these residual based approaches are now standard in finite elements because they are more mathematically sound, more precise and allow to compute upper and lower bounds for energy norms as well as functional outputs.

In this paper the implicit residual-type flux-free error estimator proposed in [23], which has similar efficiency as standard hybrid-flux estimators, is extended to the Element Free Galerkin Method. The remainder of the paper is structured as follows. Section 2, following [23], recalls the basics on output oriented error estimation in finite elements and introduces a flux-free error estimator. Section 3 is devoted to extend step by step the previous concepts to the Element Free Galerkin method: Dirichlet boundary conditions, definition of the reference error, estimation of outputs of interest, numerical integration, local domain for the error equation, and finally the solvability of the local problems. Finally, in Section 4, some numerical examples are shown.

2 Basics on output oriented error estimation in FEM

2.1 Model Problem

Let $\Omega \subset \mathbb{R}^{\mathtt{n_{sd}}}$ be an open, bounded domain with piecewise linear boundary $\partial\Omega$ and $\mathtt{n_{sd}}$ the number of spatial dimensions. The scalar strong form of the problem is: find u such that

$$\begin{cases} -\boldsymbol{\nabla}^2 u + \sigma u = s & \text{in } \Omega, \\ u = u_D & \text{on } \partial\Omega. \end{cases} \tag{1}$$

Only Dirichlet boundary conditions are considered for simplicity. It is trivial to extend these concepts to account also for Neumann-type boundary conditions. The standard weak solution of this problem is $u \in \mathcal{U}$ verifying

$$a(u,v) = l(v) \quad \forall v \in \mathcal{V}, \tag{2}$$

where

$$a(u,v) = \int_\Omega \boldsymbol{\nabla} v \cdot \boldsymbol{\nabla} u + \sigma v u \, d\Omega, \quad l(v) = \int_\Omega v s \, d\Omega.$$

The usual solution and test spaces are defined $\mathcal{U} = \{u \in \mathcal{H}^1(\Omega), u|_{\partial\Omega} = u_D\}$ and $\mathcal{V}_0 = \{v \in \mathcal{H}^1(\Omega), v|_{\partial\Omega} = 0\}$, where $\mathcal{H}^1$ is the standard Sobolev space of square integrable functions and first derivatives. The bilinear form $a(\cdot,\cdot)$ induces the energy norm, which is denoted by $\|\cdot\|$, that is, $\|v\|^2 = a(v,v)$.

The finite element interpolation spaces $\mathcal{U}^H \subset \mathcal{U}$ and $\mathcal{V}_0^H \subset \mathcal{V}_0$ are associated with a finite element mesh of characteristic size H and degree p for the complete interpolation polynomial base. The geometric support of the elements for a given mesh are open subdomains denoted by Ω_k, $k = 1 \ldots \mathtt{n_{el}}$, where $\overline{\Omega} = \bigcup_k \overline{\Omega}_k$. It is also assumed that different elements do not overlap, that is, $\Omega_k \cap \Omega_l = \emptyset$ for $k \neq l$. Then, the finite element solution u_H which is an approximation to u, lies in the finite dimensional space $\mathcal{U}^H$ and verifies

$$a(u_H, v) = l(v) \quad \forall v \in \mathcal{V}_0^H.$$

2.2 Error equations and reference error

The goal of a posteriori error estimation is to assess the accuracy of the finite element solution u_H, that is, to evaluate and measure the error, $e := u - u_H$, which belongs to $\mathcal{V}$, either in the energy norm $\|e\|$ or in a quantity of interest as it will be shown next. The equation for the error is recovered from (2) replacing the exact solution u by $u_H + e$ and using the linearity of the first argument of $a(\cdot,\cdot)$

$$a(e,v) = l(v) - a(u_H, v) =: R^P(v) \quad \forall v \in \mathcal{V}_0, \tag{3}$$

where $R^P(\cdot)$ stands for the weak residue associated to the finite element approximation u_H.

The exact error e is replaced by a reference error, e_h, lying in a finite dimensional space $\mathcal{V}_0^h$ much richer than the original finite element space $\mathcal{V}_0^H$, i.e. $\mathcal{V}_0^H \subset \mathcal{V}_0^h \subset \mathcal{V}_0$. That is, the exact solution u is replaced by the reference (or truth) solution u_h; consequently, $u \approx u_h = u_H + e_h$. Given this definition of e_h it is easy to verify that the reference error is the projection of the exact error into the reference space, that is, $e_h \in \mathcal{V}_0^h$ is the solution of the problem

$$a(e_h, v) = R^P(v) \quad \forall v \in \mathcal{V}_0^h. \tag{4}$$

Direct evaluation of e_h is computationally unaffordable because the size of the system of equations is the dimension of $\mathcal{V}_0^h$. The idea behind any implicit residual error estimator is to solve local problems instead of the global problem (4). Each of these local problems require proper boundary conditions in order to obtain a good approximation of the error and to ensure solvability.

2.3 Estimation of outputs of interest

The actual interest is to bound output quantities $l^{\mathcal{O}}(u)$, where $l^{\mathcal{O}}(\cdot)$ is a linear functional, see for instance [21, 17, 25, 20, 24, 29]. These strategies introduce a dual (or adjoint) problem with respect to the selected output. The weak form of the dual problem reads: find $\psi \in \mathcal{V}_0$ such that

$$a(v, \psi) = l^{\mathcal{O}}(v) \quad \forall v \in \mathcal{V}_0.$$

The finite element approximation of the dual problem is $\psi_H \in \mathcal{V}_0^H$ such that

$$a(v, \psi_H) = l^{\mathcal{O}}(v) \quad \forall v \in \mathcal{V}_0^H.$$

Finally, the dual reference error is $\epsilon_h := \psi_h - \psi_H \ \in \mathcal{V}_0^h$, such that

$$a(v, \epsilon_h) = l^{\mathcal{O}}(v) - a(v, \psi_H) =: R^D(v) \quad \forall v \in \mathcal{V}_0^h, \tag{5}$$

where R^D is the weak residue associated with ψ_H.

If v is replaced by e_h in (5), then using Galerkin orthogonality and the parallelogram identity, the following representation of $l^{\mathcal{O}}(e_h)$ can be obtained

$$l^{\mathcal{O}}(e_h) = a(e_h, \epsilon_h) = \frac{1}{4}\|\kappa e_h + \frac{1}{\kappa}\epsilon_h\|^2 - \frac{1}{4}\|\kappa e_h - \frac{1}{\kappa}\epsilon_h\|^2 \tag{6}$$

for any arbitrary scalar parameter κ. To simplify the notation the arguments in the squared norms of the r.h.s. in (6) are denoted by $z_h^{\pm} = \kappa e_h \pm \frac{1}{\kappa}\epsilon_h$.

In fact, in order to bound the output of the error, $l^{\mathcal{O}}(e_h)$, the r.h.s of (6) indicates that it is sufficient to bound the energy norm of z_h^+ and z_h^-, (i.e. the energy norm of linear combinations of e_h and ϵ_h).

Define $\mathrm{E_u}[v]$ and $\mathrm{E_l}[v]$ as the upper and lower bound of $\|v\|^2$, respectively. Note that $\mathrm{E_u}[v]$ and $\mathrm{E_l}[v]$ are not functions; instead, it is a convenient notation of the bounds. Thus, once the bounds for $\|z_h^{\pm}\|^2$ are computed, namely $\mathrm{E_l}[z_h^{\pm}] \leq \|z_h^{\pm}\|^2 \leq \mathrm{E_u}[z_h^{\pm}]$, the output of the error is readily bounded as

$$\frac{1}{4}\mathrm{E_l}[z_h^+] - \frac{1}{4}\mathrm{E_u}[z_h^-] \leq l^{\mathcal{O}}(e_h) \leq \frac{1}{4}\mathrm{E_u}[z_h^+] - \frac{1}{4}\mathrm{E_l}[z_h^-], \tag{7}$$

and, obviously, the bounds for the output of interest of the reference approximation, $l^{\mathcal{O}}(u_h)$, are

$$l^{\mathcal{O}}(u_H) + \frac{1}{4}\mathrm{E_l}[z_h^+] - \frac{1}{4}\mathrm{E_u}[z_h^-] \leq l^{\mathcal{O}}(u_h) \leq l^{\mathcal{O}}(u_H) + \frac{1}{4}\mathrm{E_u}[z_h^+] - \frac{1}{4}\mathrm{E_l}[z_h^-].$$

Next section introduces a methodology to obtain both upper and lower bound error estimates in energy norm. This approach is then used to compute $\mathrm{E_u}[z_h^+]$, $\mathrm{E_u}[z_h^-]$, $\mathrm{E_l}[z_h^+]$ and $\mathrm{E_l}[z_h^-]$.

2.4 Upper bound estimate of the reference error

Let $\boldsymbol{x}^i$, $i = 1, \ldots, \mathtt{n_{np}}$ denote the vertices of the elements in the computational mesh (thus linked to $\mathcal{U}^H$) and ϕ^i the corresponding linear (or bilinear or trilinear) shape functions, which are such that $\phi^i(\boldsymbol{x}^j) = \delta_{ij}$. The support of ϕ^i is denoted by ω^i and it is called the star centered in, or associated with, vertex $\boldsymbol{x}^i$.

It is important to recall that the linear shape functions based on the vertices are a *partition of unity*. Using this essential property and the linearity of the weak residue $R^P(\cdot)$, defined in (3), the residue is decomposed into local contributions over each star

$$R^P(v) = R^P\Big(\sum_{i=1}^{\mathtt{n_{np}}} \phi^i v\Big) = \sum_{i=1}^{\mathtt{n_{np}}} R^P(\phi^i v) \quad \forall v \in \mathcal{H}^1(\Omega).$$

Note that $R^P(\phi^i v)$ vanishes if $\operatorname{supp} v \cap \omega^i = \emptyset$, since ω^i is the support of ϕ^i.

The strategy to compute upper bound estimates of the reference error, $\mathrm{E_u}[e_h]$, consist in, first, the evaluation of the finite element solution u_H, which is necessary to compute the residue R^P. And, second, the appraisal of the local estimates $\tilde{e}^{\omega^i} \in \mathcal{V}^h_{\omega^i}$, where $\mathcal{V}^h_{\omega^i} := \mathcal{V}^h_0 \cap \mathcal{H}^1(\omega^i)$, solving problems in each star ω^i

$$a_{\omega^i}(\tilde{e}^{\omega^i}, v) = R^P(\phi^i v) \quad \forall v \in \mathcal{V}^h_{\omega^i}, \tag{8}$$

where $a_{\omega^i}(\cdot,\cdot)$ is the restriction of the bilinear form $a(\cdot,\cdot)$ to the star ω^i.

Remark 1. Formally any function $v \in \mathcal{V}^h_{\omega^i}$ is not defined in the whole domain Ω but only in the star ω^i. However, here every $v \in \mathcal{V}^h_{\omega^i}$ is naturally extended to Ω by setting its value outside ω^i equal to zero. Thus, functions in $\mathcal{V}^h_{\omega^i}$ are continuous in ω^i but generally discontinuous across the boundary of the star.

Remark 2. The local restriction $\mathcal{V}^h_0$ to the element Ω_k, $\mathcal{V}^h_{\Omega_k} := \mathcal{V}^h_0 \cap \mathcal{H}^1(\Omega_k)$, is also extended to Ω in the same way. This induces the *broken space*, namely

$$\mathcal{V}^h_{\mathrm{brok}} := \bigoplus_{k=1}^{\mathtt{n_{el}}} \mathcal{V}^h_{\Omega_k}.$$

Note that functions in $\mathcal{V}^h_{\text{brok}}$ may present discontinuities across the inter-element edges (or faces) and that $\mathcal{V}^h_{\omega^i} \subset \mathcal{V}^h_{\text{brok}}$.

Remark 3. The bilinear form $a(\cdot,\cdot)$ and the energy norm are generalized to accept *broken* functions in its arguments; that is, for v and $w \in \mathcal{V}^h_{\text{brok}}$,

$$a(v,w) := \sum_{k=1}^{\mathtt{n_{el}}} a_{\Omega_k}(v,w) \quad \text{and} \quad \|v\|^2 := \sum_{k=1}^{\mathtt{n_{el}}} \|v\|^2_k,$$

where $a_{\Omega_k}(\cdot,\cdot)$ is the restriction of the bilinear form $a(\cdot,\cdot)$ to the element Ω_k and $\|v\|^2_k = a_{\Omega_k}(v,v)$.

Finally, adding the local estimates, which have been extended into $\mathcal{V}^h_{\text{brok}}$, a global estimate $\tilde{e} \in \mathcal{V}^h_{\text{brok}}$ is obtained,

$$\tilde{e} := \sum_{i=1}^{\mathtt{n_{np}}} \tilde{e}^{\omega^i},$$

and the upper bound of the energy norm of the reference error is recovered computing the norm of the estimate $\tilde{e}$. See [23] for a detailed description, development and formal analysis (viz. the proof of the next theorem) of this estimator.

Theorem 1. *The estimate* $\tilde{e} = \sum_{i=1}^{\mathtt{n_{np}}} \tilde{e}^{\omega^i}$*, where* $\tilde{e}^{\omega^i}$ *is the solution of the local problem given in* (8)*, is such that*

$$\mathrm{E_u}[e_h] = \|\tilde{e}\|^2 \geq \|e_h\|^2.$$

3 Extension to Element Free Galerkin

3.1 Reference error

Similarly to finite elements, in mesh-free methods a finite dimensional space $\mathcal{V}^H \subset \mathcal{H}^1(\Omega)$ is associated with a particle distribution of characteristic size H and degree p for the reproducibility imposed. Thus, the mesh-free solution u_H, which is an approximation to u, belongs to $\mathcal{V}^H$ and verifies

$$a(u_H, v) = l(v) \quad \forall v \in \mathcal{V}^H.$$

However, in mesh-free methods the refined spaces are, in general, not nested, i.e. $\mathcal{V}^H \not\subset \mathcal{V}^h$. The reference error in EFG is directly defined as the projection of the exact error into the reference space, i.e. $e_h \in \mathcal{V}^h$ is the solution of

$$a(e_h, v) = R^P(v) \quad \forall v \in \mathcal{V}^h, \tag{9}$$

and, in general, $e_h \neq u_h - u_H$. This weak problem is very similar to (4) and only differs in the functional spaces because Dirichlet boundary conditions are imposed differently. This issue will be addressed in Section 3.6. It is important to emphasize that in mesh-free methods the reference error is not anymore $u_h - u_H$ as in finite elements but only the solution of problem (9).

3.2 Estimation of outputs of interest

When bounds for outputs are sought, as in finite elements —recall equation (5)—, a dual reference error is defined as $\epsilon_h \in \mathcal{V}^h$ solution of

$$a(v, \epsilon_h) = l^{\mathcal{O}}(v) - a(v, \psi_H) =: R^D(v) \quad \forall v \in \mathcal{V}^h. \tag{10}$$

Note again, that also in this case $\epsilon_h \neq \psi_h - \psi_H$. If v is replaced by e_h in (10),

$$l^{\mathcal{O}}(e_h) = a(e_h, \epsilon_h) + a(e_h, \psi_H). \tag{11}$$

In finite elements Galerkin orthogonality implies $a(e_h, \psi_H) = 0$ but not in EFG. Nevertheless, the first term in the r.h.s. of (11) can be rewritten using the parallelogram identity —as in section 2.3 and equation (6)—, namely,

$$l^{\mathcal{O}}(e_h) = \frac{1}{4}\|\kappa e_h + \frac{1}{\kappa}\epsilon_h\|^2 - \frac{1}{4}\|\kappa e_h - \frac{1}{\kappa}\epsilon_h\|^2 + a(e_h, \psi_H).$$

Thus in EFG the output of the error, see (7), is bounded by

$$\frac{1}{4}\mathrm{E_l}[z_h^+] - \frac{1}{4}\mathrm{E_u}[z_h^-] + a(e_h, \psi_H) \leq l^{\mathcal{O}}(e_h) \leq \frac{1}{4}\mathrm{E_u}[z_h^+] - \frac{1}{4}\mathrm{E_l}[z_h^-] + a(e_h, \psi_H). \tag{12}$$

Several alternatives are possible to cope with the extra term, $a(e_h, \psi_H)$, in EFG. The simplest one is to neglect it because intuitively it is expected to be small. Another alternative is to compute bounds for it. Here, however, it will be evaluated using a computable high-order approximation, thus introducing an error which is negligible in front of the other terms.

3.3 Upper bound estimate of the reference error

In EFG the upper estimate of the reference error can also be computed with the same rationale as in finite elements. The partition of unity is naturally induced by the *moving least squares* interpolating function, which are also denoted as ϕ^i (i now being the index of each particle). Similar restriction of the functional spaces are defined, that is

$$\mathcal{V}^h_{\omega^i} := \mathcal{V}^h \cap \mathcal{H}^1(\omega^i), \quad \mathcal{V}^h_{\Omega_k} := \mathcal{V}^h \cap \mathcal{H}^1(\Omega_k), \text{ and } \mathcal{V}^h_{\text{brok}} := \bigoplus_{k=1}^{\mathtt{n_{el}}} \mathcal{V}^h_{\Omega_k}.$$

And the estimate also verifies equation (8), namely, find $\tilde{e}^{\omega^i} \in \mathcal{V}^h_{\omega^i}$ solving the local problems in each star ω^i

$$a_{\omega^i}(\tilde{e}^{\omega^i}, v) = R^P(\phi^i v) \quad \forall v \in \mathcal{V}^h_{\omega^i}. \tag{8}$$

Thus the estimate

$$\tilde{e} := \sum_{i=1}^{\mathtt{n_{np}}} \tilde{e}^{\omega^i}, \tag{13}$$

and the upper bound of the energy norm of the reference error is recovered computing the norm of the estimate $\tilde{e}$. Because theorem 1 is also applicable here since it is based on the following lemma, which characterizes this broken approximation.

Lemma 1. *Any estimate* $\tilde{e} \in \mathcal{V}^h_{\text{brok}}$ *verifying the weak error equation*

$$a(\tilde{e}, v) = R^P(v) \quad \forall v \in \mathcal{V}^h, \tag{14}$$

is such that the norm of $\tilde{e}$ *is an upper bound of the energy norm of the reference error, that is*

$$\|\tilde{e}\|^2 \geq \|e_h\|^2.$$

From practical point of view, to reduce drastically the computational effort and in order to simplify the evaluation of the local estimates, equation (8), the definition of the star ω^i is modified. Figure 1 illustrates the definition of the star ω^i. Recall that a local problem is solved in each star and that ϕ^i is extended (equal to zero) outside of ω^i.

Definition 1. *A star,* ω^i*, is the smallest integration sub-grid that includes the support of* ϕ^i*.*

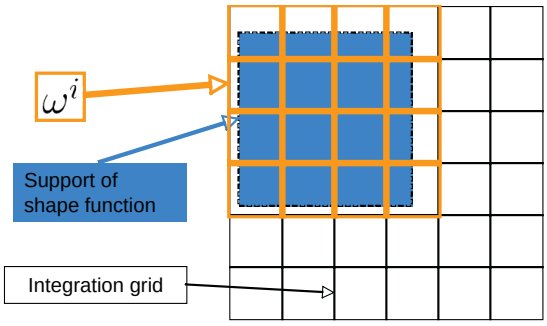

Figure 1. Definition of the star ω^i.

Remark 4. The solvability of the local problem, equation (8), is ensured in scalar problems as the kernel of $a_{\omega^i}(w, \cdot)$ for a generic function w includes only constant functions and for v constant the r.h.s is zero by Galerkin orthogonality, i.e. $R^P(\phi^i v) = 0$ for v constant.

3.4 Evaluation of bounds for the outputs

As noted in section 3.2 the bounds for the output of interest in EFG introduce a new term $a(e_h, \psi_H)$, which in principle is unknown. Here, a high-order approximation is proposed.

Theorem 2. *The term $a(\tilde{e}, \psi_H)$, where $\tilde{e}$ is given by 13 and ψ_H is the coarse solution of the dual (adjoint) problem, is a high-order approximation of $a(e_h, \psi_H)$. In fact,*

$$|a(e_h, \psi_H) - a(\tilde{e}, \psi_H)| \leq C\, h^p H^p. \tag{15}$$

Proof. In view of the definition of the reference error (9) and the properties of the estimator, see equation (14), it is known that,

$$R^P(v) = a(e_h, v) = a(\tilde{e}, v) \quad \forall v \in \mathcal{V}^h,$$

and therefore, $a(e_h - \tilde{e}, \boldsymbol{\pi}^h \psi_H) = 0$. Where the interpolation operator of any function in $\mathcal{V}$ onto the the reference space, $\mathcal{V}^h$, is introduced. That is, $\boldsymbol{\pi}^h : \mathcal{V} \longrightarrow \mathcal{V}^h$ is such that $\boldsymbol{\pi}^h v(\boldsymbol{x}^i) = v(\boldsymbol{x}^i)$ where $\boldsymbol{x}^i$ denote the nodes (particles) of the reference mesh. Thus,

$$a(e_h - \tilde{e}, \psi_H) = a(e_h - \tilde{e}, \psi_H - \boldsymbol{\pi}^h \psi_H)$$

which induces the following bound after using Cauchy-Schwartz inequality

$$|a(e_h - \tilde{e}, \psi_H)| = |a(\tilde{e} - e_h, \psi_H - \boldsymbol{\pi}^h \psi_H)| \leq \|e_h - \tilde{e}\| \|\psi_H - \boldsymbol{\pi}^h \psi_H\|.$$

In order to finish the proof the standard interpolation error is employed, i.e. $\|\psi_H - \boldsymbol{\pi}^h \psi_H\| \leq C_1 h^p$, and the bound $\|e_h - \tilde{e}\| \leq C_2 H^p$ is recalled. The latter bound requires that the estimator is efficient (i.e. that exists a constant, $C_3 \leq 1$ such that $C_3 \|\tilde{e}\| \leq \|e_h\| \leq \|\tilde{e}\|$) to obtain the following bound

$$\begin{aligned}
\|e_h - \tilde{e}\|^2 &= \|e_h\|^2 + \|\tilde{e}\|^2 - 2a(e_h, \tilde{e}) \\
&= \|e_h\|^2 + \|\tilde{e}\|^2 - 2R^P(e_h) \\
&= \|e_h\|^2 + \|\tilde{e}\|^2 - 2\|e_h\|^2 \\
&= \|\tilde{e}\|^2 - \|e_h\|^2 \leq \frac{1}{C_3}\|e_h\|^2 - \|e_h\|^2 = (\frac{1}{C_3} - 1)\|e_h\|^2.
\end{aligned}$$

Using now the standard approximation bound $\|e_h\| \leq \|e\| = \|u - u_H\| \leq C_4 H^p$ in the previous equation the desired result $\|e_h - \tilde{e}\| \leq C_2 H^p$ is obtained to end the proof.

□

Thus, in practice, the bounds for the output of the error presented in equation (12) are computed using

$$\frac{1}{4}\mathrm{E_l}[z_h^+] - \frac{1}{4}\mathrm{E_u}[z_h^-] + a(\tilde{e}, \psi_H) \leq l^{\mathcal{O}}(e_h) \leq \frac{1}{4}\mathrm{E_u}[z_h^+] - \frac{1}{4}\mathrm{E_l}[z_h^-] + a(\tilde{e}, \psi_H),$$

and, obviously, the bounds for the output of interest of the reference approximation, $l^{\mathcal{O}}(u_h)$, are

$$\begin{aligned}
l^{\mathcal{O}}(u_h) &\geq l^{\mathcal{O}}(u_H) + \frac{1}{4}\mathrm{E_l}[z_h^+] - \frac{1}{4}\mathrm{E_u}[z_h^-] + a(\tilde{e}, \psi_H) \\
l^{\mathcal{O}}(u_h) &\leq l^{\mathcal{O}}(u_H) + \frac{1}{4}\mathrm{E_u}[z_h^+] - \frac{1}{4}\mathrm{E_l}[z_h^-] + a(\tilde{e}, \psi_H).
\end{aligned}$$

3.5 Numerical integration

Suppose the coarse (global) problem is solved with a given numerical quadrature,

$$a_Q(u_H, v) = l_Q(v) \quad \forall v \in \mathcal{V}^H.$$

Then, as expected, the residue is zero,

$$R_Q^P(v) = l_Q(v) - a_Q(u_H, v) = 0 \quad \forall v \in \mathcal{V}^H.$$

But for a different quadrature,

$$a_q(u_H, v) \neq l_q(v) \quad \forall v \in \mathcal{V}^H,$$

and, thus, Galerkin orthogonality is lost,

$$R_q^P(v) = l_q(v) - a_q(u_H, v) \neq 0 \quad \forall v \in \mathcal{V}^H.$$

Therefore, the same quadrature must be used to compute on the coarse and reference (truth) discretizations because Galerkin orthogonality is needed both (theoretically) to proof the upper bound property and also (practically) to ensure solvability of the local problems, see remark 4. This obviously implies that the so-called "coarse" computation is done with the quadrature of the reference discretization. This is obviously and extra cost which is required to compute the error distribution. This, however, does not preclude any adaptive refinement scheme as it will be seen in the next section.

3.6 Dirichlet boundary conditions

In the mesh-free context, shape functions usually do not verify the Kronecker delta property. Therefore, imposing Dirichlet boundary conditions is not as trivial as in the finite element method. In recent years, many specific techniques for the implementation of essential boundary conditions in mesh-free methods have been developed. A general overview on existing techniques is presented in [9]. Of the different techniques discussed in [9] the continuous blending method [12, 13, 8] (i.e. introduce standard finite elements along the boundary and adapt the mesh-free interoplation functions to obtain completeness) and Nitsche's method [19, 27, 2] are the most suitable alternatives. Both alternatives can be used to estimate the error. Here, for compactness of the notation Nitsche's method is used to define the weak form and has been used the examples.

The weak solution of problem (1) requires to find $u \in \mathcal{H}^1(\Omega)$ verifying

$$a(u, v) = l(v) \quad \forall v \in \mathcal{H}^1(\Omega), \tag{16}$$

where Nitsche's method modifies the forms in the previous equation as follows:

$$a(u,v) = \int_\Omega \boldsymbol{\nabla} v \cdot \boldsymbol{\nabla} u + \sigma v u \, d\Omega - \int_{\partial\Omega} v \, \boldsymbol{n} \cdot \boldsymbol{\nabla} u \, d\Gamma - \int_{\partial\Omega} u \, \boldsymbol{n} \cdot \boldsymbol{\nabla} v \, d\Gamma + \beta \int_{\partial\Omega} v u \, d\Gamma, \quad (17)$$

$$l(v) = \int_\Omega v s \, d\Omega - \int_{\partial\Omega} u_D \, \boldsymbol{n} \cdot \boldsymbol{\nabla} v \, d\Gamma + \beta \int_{\partial\Omega} v u_D \, d\Gamma. \quad (18)$$

Note that equation (16) is identical to (2) but the spaces for the approximation and the test functions are different. Note also that as in finite elements, this bilinear form $a(\cdot,\cdot)$ also induces an energy norm.

The last term in (17) is required to ensure coercivity of the bilinear form $a(\cdot,\cdot)$ provided that β is large enough. Regarding the choice of the lower bound of β, Nitsche proved that if β is taken as $\beta = \gamma/\ell$, where γ is a large enough constant (independent of h) and ℓ denotes a characteristic measure of the finite element discretization, then the discrete solution converges to the exact solution with optimal order in $\mathcal{H}^1$ and $\mathcal{L}^2$ norms. Moreover, γ can be estimated from the maximum eigenvalue of a generalized eigenvalue problem, see [11]. Similar results are obtained for mesh-free methods and ℓ is related to a measure of the support of the interpolation functions or equivalently to the distance between particles.

Here, two characteristic sizes are used, H is associated to the coarse discretization and h characterizes the reference or truth distribution of particles. As in the previous section *only one* bilinear form is used. Thus $a(\cdot,\cdot)$, and consequently β, is the same for both the global coarse computation in $\mathcal{V}^H$and the local reference evaluation in $\mathcal{V}^h$. This obviously implies choosing for β the corresponding value associated to the reference mesh (as already done in the numerical integration). Because it will be larger than the one related to $\mathcal{V}^H$and thus will ensure coercivity of (17) and obviously consistency of (16).

In summary, as for numerical integration, the parameter β used in the coarse distribution of particles is associated to the reference distribution used later to evaluate the error distribution. Again, this is necessary both for theoretical and practical considerations (Galerkin orthogonality is necessary). Nevertheless, this does not preclude any adaptive scheme, as will be shown on a following publication, because at each refinement step the reference distribution of particles is known a priori (it is directly related to the given "coarse" distribution of particles).

4 Numerical results

In this section, the proposed estimator is used to evaluate bounds for thermal model problems. Some of the selected examples have been used by other authors to assess the performance of similar techniques [23, 20].

4.1 First Poisson example

The 2D Laplace problem

$$\begin{cases} \boldsymbol{\nabla}^2 u = 0 & \text{in } (x,y) \in]0,1[\times]0,1[\\ u(x,0) = \sin(\pi x) & \\ u(x,1) = u(0,y) = u(1,y) = 0 & \end{cases}$$

with known analytical solution [28, 9],

$$u(x,y) = \big(\cosh(\pi y) - \coth(\pi)\sinh(\pi y)\big)\sin(\pi x),$$

is considered next. Figure 2 shows this analytical solution and the primal and dual approximations using EFG with bilinear consistency and a uniform distribution of particles of 5×5.

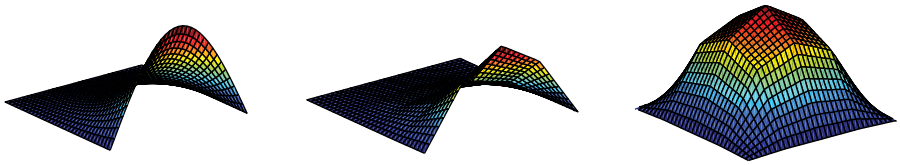

Figure 2. Exact solution (left), EFG primal (center) and dual (right) approximations.

The behavior of the energy norm estimate is compared to the exact energy error norm and the reference error energy norm, see Figure 3. The approximate solution u_H is computed using bilinear consistency and the reference space is associated with a particle distribution $h = H/4$. Uniform distributions of particles have been considered. From a qualitative viewpoint, it is worth noting that the estimated error distribution is in good agreement with the exact error distribution.

Figure 4 shows the spatial distribution of the local effectivity index. It is important to notice that the effectivity index is always close to the optimum value: one. Obviously if the index is evaluated using the reference error, e_h, which is the value actually bounded, the effectivity index is even better (closer to one and more uniform).

Remark 5. Elements of the integration grid with very small contributions to the errors are not considered in the previous plot (areas not plotted) because they are not interesting from an adaptive viewpoint. Moreover, in these areas, small roundoff errors in the error assessment lead to unreasonable effectivity indices (very small absolute error but large relative error). An element is considered to have a "small" contribution to the global error when $\|e_h\|/4n_{el}$ (with n_{el} being the number of elements of the integration grid). This results, in this case, on neglecting 20% of the elements approximately.

Remark 6. The local energy norm has been represented in the integration grid. From now on, all local representations will be represented in this grid.

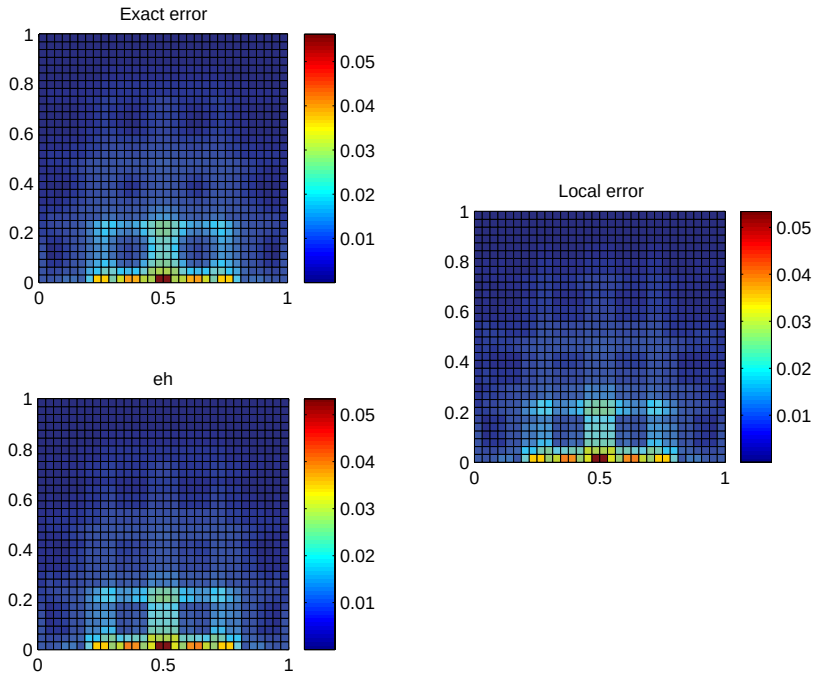

Figure 3. Energy norm of error and estimate.

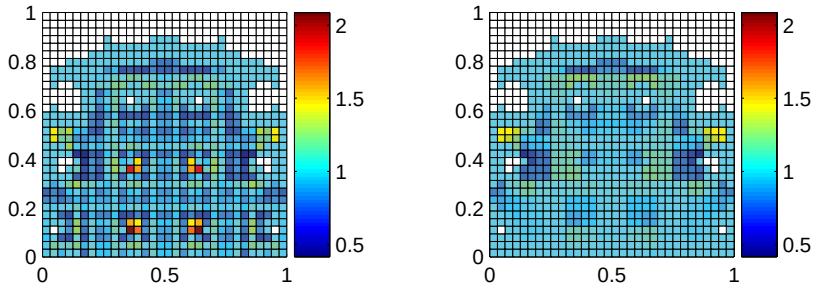

Figure 4. Local effectivity index with respect exact error (left) and with respect the reference error, e_h, (right).

Finally, Figure 5 shows the resulting bounds and their convergence. The lower and upper bounds for an approximation to the output of the exact solution are shown as well as the bound average, the EFG approximation and the exact output. As expected they converge to the exact output as the number

of particles is refined. Second order convergence is obtained as bilinear consistency is used. For the initial distribution of particles (uniform distribution

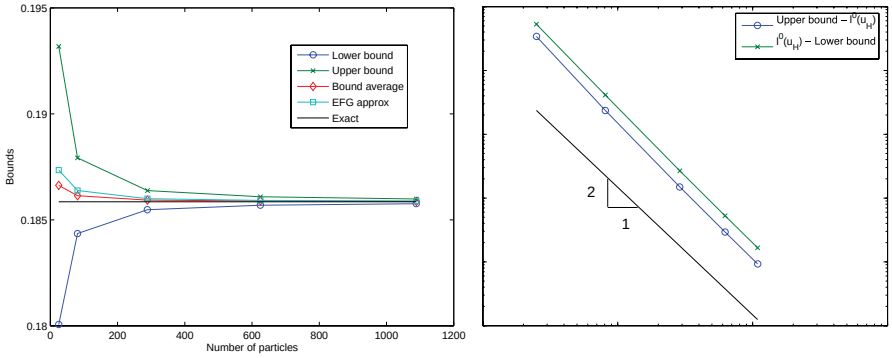

Figure 5. Resulting bounds (left) and their convergence (right).

of 5×5 particles) the output is bounded by, $l^{\mathcal{O}}(u_h) \in [0.1801, 0.1932]$, that is

$$l^{\mathcal{O}}(u_h) = 0.1866 \pm 0.0066 = 0.1866 \pm 3.54\%$$

and for the final distribution (33×33 particles) the output is bounded by $l^{\mathcal{O}}(u_h) \in [0.1858, 0.1860]$

$$l^{\mathcal{O}}(u_h) = 0.1859 \pm 0.0001 = 0.1859 \pm 0.05\%.$$

4.2 Second Poisson example

A well-known benchmark is solved in this section, see [1, 20, 6, 23]. The problem reads,

$$\begin{cases} -\boldsymbol{\nabla}^2 u = s & \text{in } \Omega, \\ u = 0 & \text{on } \partial\Omega, \end{cases}$$

where the source term is chosen such that the exact solution has the following analytical expression

$$u(x, y) = x^2(1-x)^2(e^{10x^2} - 1)y^2(1-y)^2(e^{10y^2} - 1)/2000.$$

Figure 6 shows this analytical solution and the primal and dual approximations using EFG with bilinear consistency and a uniform distribution of particles of 5×5. Note that the EFG primal solution verifies the Dirichlet boundary condition weakly as expected when it is imposed by Nitsche's method.

The behavior of the energy norm estimate is compared to the exact energy error norm and the reference error energy norm, see Figure 7. The approximate

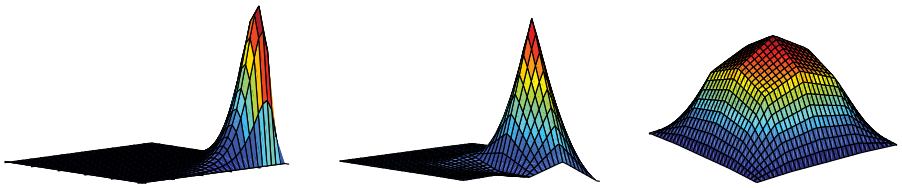

Figure 6. Exact solution (left), EFG primal (center) and dual (right) approximations.

solution u_H is computed using bilinear consistency and the reference space is associated with a particle distribution $h = H/4$. Uniform distributions of particles have been considered. From a qualitative viewpoint, it is worth noting that also in this example the estimated error distribution is in good agreement with the exact error distribution and almost identical to the reference error distribution. In fact, this comparison is more clear in Figure 8 where the spatial distribution of the local effectivity indexes is plotted.

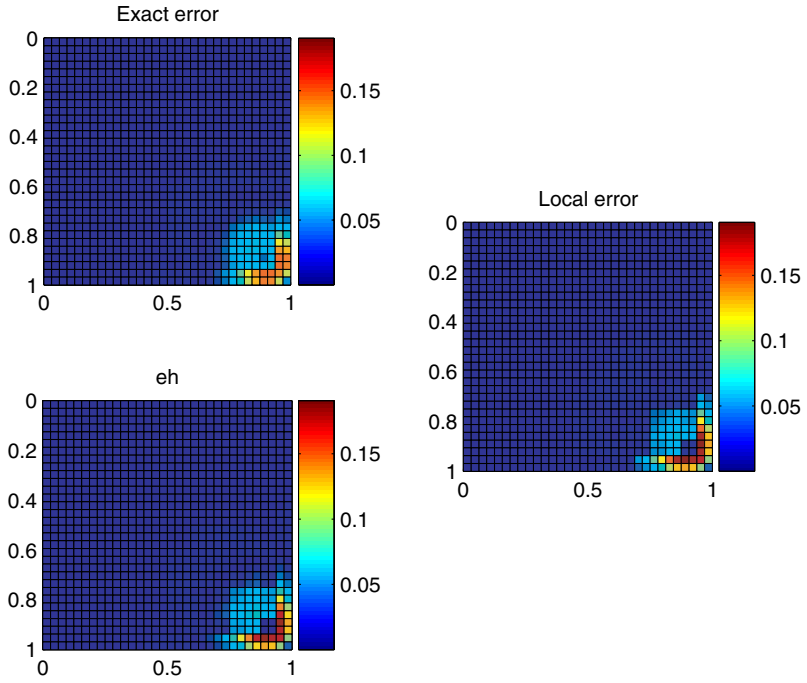

Figure 7. Energy norm of error and estimate.

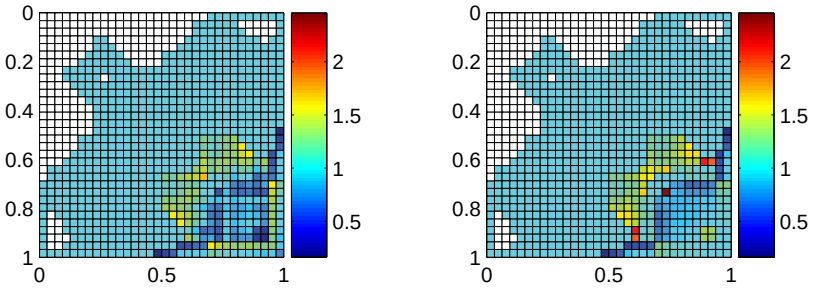

Figure 8. Local effectivity index with respect exact error (left) and with respect e_h (right).

Finally, Figure 9 shows the resulting bounds and their convergence. The lower and upper bounds for an approximation to the output of the exact solution are shown as well as the bound average, the EFG approximation and the exact output. As expected the optimal rete of converge is obtained as the number of particles is refined.

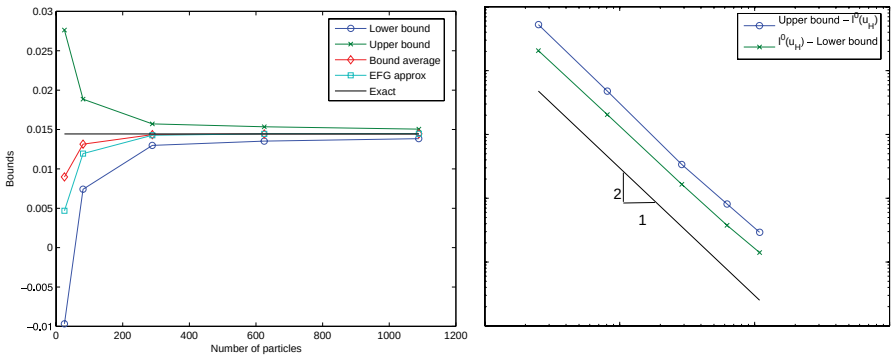

Figure 9. Resulting bounds and their convergence.

For the initial distribution of particles (uniform distribution of 5×5 particles) the output is bounded by, $l^{\mathcal{O}}(u_h) \in [-0.0097, 0.0276]$

$$l^{\mathcal{O}}(u_h) = 0.0090 \pm 0.0187 = 0.0090 \pm 207.78\%$$

and for the final distribution (33×33 particles) the output is bounded by $l^{\mathcal{O}}(u_h) \in [0.0138, 0.0150]$

$$l^{\mathcal{O}}(u_h) = 0.0144 \pm 0.0006 = 0.0144 \pm 4.17\%.$$

5 Concluding remarks

For the first time in mesh-free methods an implicit residual-based estimation is presented. Moreover, with this strategy bounds for outputs of interest can be computed. The resulting estimate yields upper and lower bounds for the output of the reference error. Moreover, the distribution of local contributions to the error are accurately estimated, both for the energy norm of the error and for the error measured using some functional output. Therefore, this estimate is well suited to guide goal-oriented adaptive procedures.

References

1. M. Ainsworth and J.T. Oden, *A posteriori error estimation in finite element analysis*, John Wiley & Sons, Chichester, 2000.
2. R. Becker, *Mesh adaptation for Dirichlet flow control via Nitsche's method*, Commun. Numer. Methods Eng. **18** (2002), no. 9, 669–680.
3. J. Bonet, A. Huerta, and J. Peraire, *The efficient computation of bounds for functionals of finite element solutions in large strain elasticity*, Comput. Methods Appl. Mech. Engrg. **191** (2002), no. 43, 4807–4826.
4. C. Carstensen and S.A. Funken, *Fully reliable localized error control in the FEM*, SIAM J. Sci. Comput. **21** (1999/00), no. 4, 1465–1484.
5. H.J. Chung and T. Belytschko, *An error estimate in the EFG method*, Comput. Mech. **21** (1998), no. 2, 91–100.
6. P. Diez, N. Pares, and A. Huerta, *Recovering lower bounds of the error by post-processing implicit residual a posteriori error estimates*, Internat. J. Numer. Methods Engrg. **56** (2003), no. 10, 1465–1488.
7. C.A. Duarte and J.T. Oden, *An h-p adaptive method using clouds*, Comput. Methods Appl. Mech. Eng. **139** (1996), no. 1-4, 237–262.
8. S. Fernandez-Mendez, J. Bonet, and A. Huerta, *Continuous blending of SPH with finite elements*, Comput. Struct. **83** (2005), no. 17–18, 1448–1458.
9. S. Fernandez-Mendez and A. Huerta, *Imposing essential boundary conditions in mesh-free methods*, Comput. Methods Appl. Mech. Eng. **193** (2004), no. 12–14, 1257–1275.
10. L. Gavete, J.L. Cuesta, and A. Ruiz, *A procedure for approximation of the error in the EFG method*, Int. J. Numer. Methods Eng. **53** (2002), 667–690.
11. M. Griebel and M.A. Schweitzer, *A Particle-Partition of Unity Method. Part V: Boundary Conditions*, Geometric Analysis and Nonlinear Partial Differential Equations, (S. Hildebrandt and H. Karcher, eds.), Springer, 2002, pp. 517–540.
12. A. Huerta and S. Fernandez-Mendez, *Enrichment and coupling of the finite element and meshless methods*, Int. J. Numer. Methods Eng. **48** (2000), no. 11, 1615–1636.
13. A. Huerta, S. Fernandez-Mendez, and W.K. Liu, *A comparison of two formulations to blend finite elements and mesh-free methods*, Comput. Methods Appl. Mech. Eng. **193** (2004), no. 12–14, 1105–1117.
14. P. Ladevèze and D. Leguillon, *Error estimate procedure in the finite element method and applications*, SIAM J. Numer. Anal. **20** (1983), no. 3, 485–509.

15. W.K. Liu, S. Jun, D.T. Sihling, Y. Chen, and W. Hao, *Multiresolution reproducing kernel particle method for computational fluid dynamics*, Int. J. Numer. Methods Fluids **24** (1997), 1391–1415.
16. L. Machiels, Y. Maday, and A.T. Patera, *A "flux-free" nodal Neumann subproblem approach to output bounds for partial differential equations*, C. R. Acad. Sci. Paris Sér. I Math. **330** (2000), no. 3, 249–254.
17. Y. Maday, A.T. Patera, and J. Peraire, *A general formulation for a posteriori bounds for output functionals of partial differential equations; application to the eigenvalue problem*, C. R. Acad. Sci. Paris Sér. I Math. **328** (1999), no. 9, 823–828.
18. P. Morin, R.H. Nochetto, and K.G. Siebert, *Local problems on stars: a posteriori error estimators, convergence, and performance*, Math. Comp. **72** (2003), no. 243, 1067–1097.
19. J. Nitsche, *über ein variations zur lösung von dirichlet-problemen bei verwendung von teilräumen die keinen randbedingungen unterworfen sind*, Abh. Math. Se. Univ. **36** (1970), 9–15.
20. J.T. Oden and S. Prudhomme, *Goal-oriented error estimation and adaptivity for the finite element method*, Comput. Math. Appl. **41** (2001), no. 5-6, 735–756.
21. M. Paraschivoiu, J. Peraire, and A.T. Patera, *A posteriori finite element bounds for linear-functional outputs of elliptic partial differential equations*, Comput. Methods Appl. Mech. Eng. **150** (1997), no. 1-4, 289–312.
22. N. Pares, J. Bonet, A. Huerta, and J. Peraire, *The computation of bounds for linear-functional outputs of weak solutions to the two-dimensional elasticity equations*, Comput. Methods Appl. Mech. Eng. **194** (2006), no. 4–6, 406–429.
23. N. Pares, P. Diez, and A. Huerta, *Subdomain-based flux-free a posteriori error estimators*, Comput. Methods Appl. Mech. Eng. **195** (2006), no. 4–6, 297–323.
24. A.T. Patera and J. Peraire, *A general Lagrangian formulation for the computation of a posteriori finite element bounds*, Error estimation and adaptive discretization methods in computational fluid dynamics, Lect. Notes Comput. Sci. Eng., vol. 25, Springer, Berlin, 2003, pp. 159–206.
25. S. Prudhomme and J.T. Oden, *On goal-oriented error estimation for elliptic problems: application to the control of pointwise errors*, Comput. Methods Appl. Mech. Eng. **176** (1999), no. 1-4, 313–331.
26. A.M. Sauer-Budge, J. Bonet, A. Huerta, and J. Peraire, *Computing bounds for linear functionals of exact weak solutions to Poisson's equation*, SIAM J. Numer. Anal. **42** (2004), no. 4, 1610–1630.
27. R. Stenberg, *On some techniques for approximating boundary conditions in the finite element method*, J. Comput. Appl. Math. **63** (1995), no. 1-3, 139–148.
28. G.J. Wagner and W.K. Liu, *Application of essential boundary conditions in mesh-free methods: a corrected collocation method*, Int. J. Numer. Methods Eng. **47** (2000), no. 8, 1367–1379.
29. Z.C. Xuan, N. Pares, and J. Peraire, *Computing upper and lower bounds for the J-integral in two-dimensional linear elasticity*, Comput. Methods Appl. Mech. Eng. **195** (2006), no. 4–6, 430–443.